JACS
JOURNAL OF THE AMERICAN CHEMICAL SOCIETY

Communication

pubs.acs.org/JACS

Visible Light-Driven Hydrogen Evolution from Water Catalyzed by A Molecular Cobalt Complex

Lianpeng Tong, Ruifa Zong, and Randolph P. Thummel*

Department of Chemistry, 112 Fleming Building, University of Houston, Houston, Texas 77204-5003, United States

Supporting Information

ABSTRACT: An approximately planar tetradentate polypyridine ligand, 8-(1″,10″-phenanthrol-2″-yl)-2-(pyrid-2′-yl)quinoline (ppq), has been prepared by two sequential Friedländer condensations. The ligand readily accommodates Co(II) bearing two axial chlorides, and the resulting complex is reasonably soluble in water. In DMF the complex shows three well-behaved redox waves in the window of 0 to −1.4 V (vs SHE). However in pH 7 buffer the third wave is obscured by a catalytic current at −0.95 V, indicating hydrogen production that appears to involve a proton-coupled electron-transfer event. The complex $[Co(ppq)Cl_2]$ (**6**) in pH 4 aqueous solution, together with $[Ru(bpy)_3]Cl_2$ and ascorbic acid as a sacrificial electron donor, in the presence of blue light (λ_{max} = 469 nm) produces hydrogen with an initial TOF = 586 h^{-1}.

Effective proton reduction is vital to a successful system for artificial photosynthesis.[1−3] While the efficiency of platinum as a proton reduction catalyst (PRC) is well-known, the scarcity of this noble metal seriously limits its widespread application. On the other hand, heterogeneous and homogeneous catalysts based on more earth-abundant cobalt have recently shown some promise as PRCs.[4,5] A family of cobalt complexes that have been extensively studied as PRCs involve a square planar tetraazamacrocycle with labile axial ligands (typically aqua or halide).[6−12] Electro- or photochemical proton reduction by these cobalt complexes was performed mostly in an organic medium at low pH rather than in neutral aqueous solution primarily due to poor solubility or instability of the complex in water or to less likely protonation by water of a reduced Co^I intermediate.[12,13] Enhancing the nucleophilicity of the Co^I center by ligand modification inevitably pushes the Co^{II}/Co^I redox couple to a more negative potential, resulting in a greater overpotential being required for catalytic proton reduction.

Compared to oxime or imine donor ligands, the pyridine moiety is more resistant to hydrogenation or hydrolysis, making it a more desirable feature in a potential PRC. In an early study it was found that $[Co(bpy)_3]^{2+}$ (bpy = 2,2′-bipyridine) is a precatalyst for H_2 evolution.[14,15] Recently several cobalt polypyridine PRCs have been developed that catalyze H_2 evolution in buffered water.[16−19] One such system, reported by Long and co-workers,[20] involves a pentapyridine ligand that is redox noninnocent in the catalytic path of H_2 evolution[21,22] such that protons are reduced at a potential where a ligand-centered redox event occurs thus avoiding the metal-centered Co^I/Co^0 redox step which often demands a more negative potential. Lau et al. have reported *trans*-$[Co(qpy)(OH_2)_2]^{2+}$ (qpy = 2,2′:6′,2″:6″,2‴-quaterpyridine) as a PRC having an equatorial qpy ligand and *trans* axial aqua ligands.[19] The role of qpy, however, was not discussed in detail.

In our laboratory we have been developing water oxidation catalysts based on polypyridine complexes of Ru(II).[23−28] A recent success has involved the complex $[Ru(dpp)(pic)_2]^{2+}$ (dpp = 2,9-di(pyrid-2′-yl)-1,10-phenanthroline and pic = 4-picoline) where the dpp binds Ru(II) as a tetradentate ligand in the equatorial plane.[29] We attempted to prepare a similar dpp complex of Co(II) but found that the smaller Co(II) ion preferred to bind dpp in a tridentate fashion, and MS analysis supported the formation of $[Co(dpp)_2]^{2+}$ in which a pendant pyridine ring on each dpp was unbound (Scheme 1).

Scheme 1

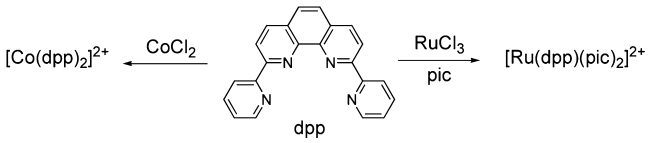

To better accommodate the smaller Co(II) ion we needed a more square planar arrangement of the tetradentate ligand. This could be accomplished by inserting an sp^2 center between the two bidentate halves of the molecule, directing us to the 8-(1″,10″-phenanthrol-2″-yl)-2-(pyrid-2′-yl)quinoline (ppq) ligand as a target. We started the synthesis of ppq by condensing 3-bromo-2-aminobenzaldehyde (**1**)[30] with 2-acetylpyridine (**2**) to afford the pyridyl bromoquinoline (**3**). Using Stille methodology we converted the bromo group to acetyl (**4**) and then carried out a second Friedländer condensation using 8-amino-7-quinolinecarbaldehyde to provide the ligand **5** (ppq) in 85% yield (Scheme 2). The extended conjugation of ppq should help to stabilize a low-valent cobalt center and favor ligand-centered reduction at a more positive potential. Furthermore, the rigid framework of ppq ensures a stable Co-ppq coordination environment and prevents dramatic distortion of the structure regardless of the valence state of the cobalt center. In addition, the planar Co-ppq motif provides open axial coordination sites for access of protons to the cobalt core. These unique features of ppq could help to provide an efficient and robust cobalt PRC.

Received: February 5, 2014
Published: March 17, 2014

   dx.doi.org/10.1021/ja501257d | *J. Am. Chem. Soc.* 2014, 136, 4881−4884

Scheme 2

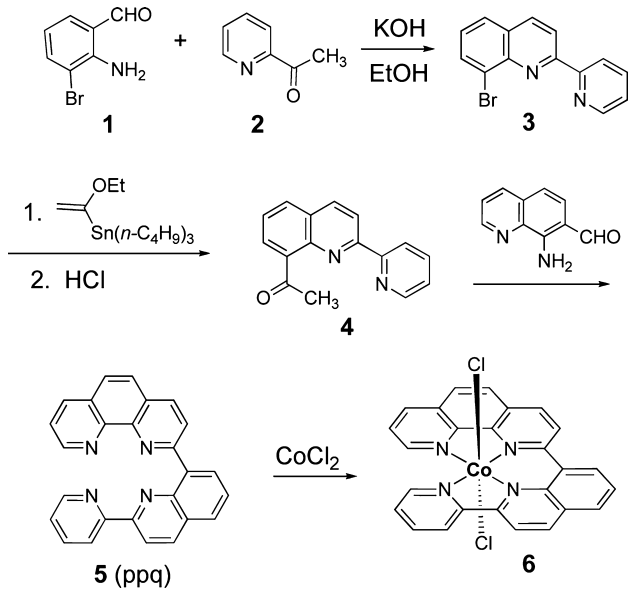

When an equimolar amount of **5** in $CHCl_3$ was combined with $CoCl_2$-$6H_2O$ in MeOH, a green solid gradually precipitated to provide a 78% yield of **6**. This material was pure by elemental analysis and showed two strong peaks in the ESI-MS (Figure S1) at m/z = 221.6 for $[Co(ppq)]^{2+}$ and 478.2 for $[Co(ppq)Cl]^{+}$. A single crystal for X-ray diffraction was grown by diffusion of diethyl ether into a DMSO solution of **6**, and an ORTEP plot of the molecule is shown in Figure 1. Pertinent geometric features are summarized in Table S2.

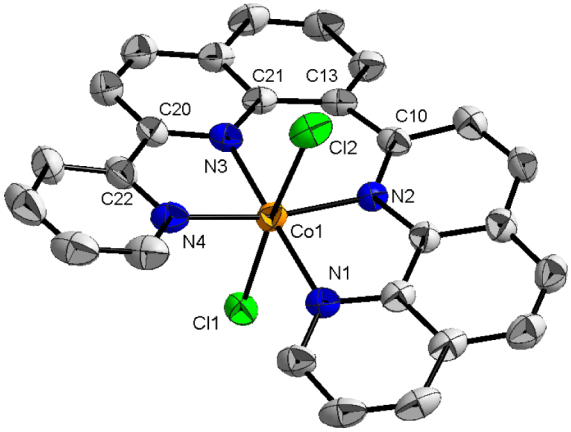

Figure 1. X-ray crystal structure of $[Co(ppq)Cl_2]$ (ellipsoids at 50% probability) with hydrogen atoms omitted for clarity. Color code: cobalt (orange), nitrogen (blue), chloride (green), and carbon (gray).

The Co−N bond lengths fall in the narrow range of 1.97−2.02 Å, slightly longer than analogous Co−N bond lengths (1.89−1.92 Å) reported for a cobalt diimine−dioxime complex having a somewhat more flexible square-planar environment in the equatorial plane.[9] Of greater interest are the Co−Cl bonds at 2.54 and 2.61 Å. These bonds are considerably longer than the axial Co−Cl bonds for the diimine-dioxime complex at 2.24 Å. These bond lengths are even longer than the Co−Cl bonds in cobalt dichloride that have been reported to range from 2.44 to 2.51 Å.[31,32] To the extent that the Co−Cl bonds have greater ionic character, they may account for better water solubility and more facile hydration, both important features for an effective homogeneous PRC. The N−Co−N bond angles of **6** are consistent with the metal ion being contained in either a five-membered (83.1° and 81.7°) or a six-membered (92.9°) chelate ring. The exterior N4−Co−N1 angle is 103.1°. The axis of Cl−Co−Cl is close to linear at 175.3° and approximately orthogonal to the equatorial plane. There is some room for distortion about the two C−C bonds of ppq. The dihedral angle about C20−C22 is 7.9°, while C10−C13 is more twisted with a dihedral angle of 19.4°. Nevertheless the sum of the four N−Co−N angles that lie in the equatorial plane is 360.8°, indicating that the ligand is reasonably planar and should afford good π-delocalization.

Complex **6** is moderately soluble in DMF and DMSO but not in other common organic solvents. It has sufficient solubility (>1 mM at 20 °C) in water for most physical measurements. The UV−vis spectra of **6** in DMF and water showed different absorption profiles (Figure S2). Considering the ionic character of the Co^{II}−Cl bond in **6**, we suggest that one or both chlorides may be replaced by water. The UV−vis spectrum of **6** in water did not change over 20 h (Figure S3) or in the presence of HCl (0.01 M, Figure S4), indicating a stable water-soluble Co^{II} species under acidic or neutral conditions. When a pH buffered aqueous solution of **6** was titrated from pH 8.6 to 11.25, a new absorption peak at 365 nm and two isosbestic points were observed (Figure S5). These observations point to the formation of a Co^{II}-aqua species which may be deprotonated under alkaline conditions.

The cyclic voltammogram (CV) of a DMF solution of **6** (Figure 2a) shows a reversible wave at $E_{1/2}$ = 0.43 V (all potentials vs SHE) which is assigned to a metal-based Co^{III}/Co^{II} redox event. Sweeping toward the cathode reveals three reversible one-electron redox waves at $E_{1/2}$ = −0.53, −0.78, and −1.13 V. For comparison, the ppq ligand in DMF displays redox waves at −1.1, −1.5, and −1.72 V (Figure S6). The first reduction wave of **6**, being 570 mV more positive than the free ligand, is assigned to a metal centered Co^{II}/Co^{I} process. The second and especially the third redox peaks, being close to the first reduction of the free ligand, are likely related to both the metal and its ppq ligand.[21,22]

We further explored the electrochemical behavior of **6** in buffered aqueous solution where pH = 2−8 which is the range associated with catalytic proton reduction. In pH 7.0 phosphate buffer, a reversible Co^{III}/Co^{II} wave at +0.57 V was observed for **6** (Figure S7). Within the pH range 3.7−9 this potential shifts linearly with pH with a slope of −59 mV/pH, indicating a proton-coupled electron-transfer process (Figure S8). This observation supports the premise that **6** hydrolyzes in water to form a $[Co^{II}(ppq)\text{-aqua}]^{2+}$ cation. Scanning cathodically in the same neutral phosphate buffer reveals a quasireversible wave at −0.4 V and an irregular wave at −0.55 V, before the onset of a catalytic current at about −0.9 V (Figure 2b and S9). The first two redox waves depicted in Figure 2b are independent of pH as demonstrated by the Pourbaix diagram (Figure S10). Therefore, proton transfer is not involved in either of these two electron-transfer steps. By analogy to the CV of **6** in DMF, these two redox waves are assigned respectively to $[Co(ppq)\text{-aqua}]^{2+}/[Co(ppq)\text{-aqua}]^{+}$ and $[Co(ppq)\text{-aqua}]^{+}/[Co(ppq)\text{-aqua}]^{0}$. The irregular shape of the second wave is attributed to the deposit of the poorly soluble $[Co(ppq)\text{-aqua}]^{0}$ on the surface of the glassy carbon electrode. When the CV was measured at scan rates of 50−800 mV/s in the range from 0 to −0.75 V, the peak current of the −0.4 V wave varied linearly

dx.doi.org/10.1021/ja501257d | J. Am. Chem. Soc. 2014, 136, 4881−4884

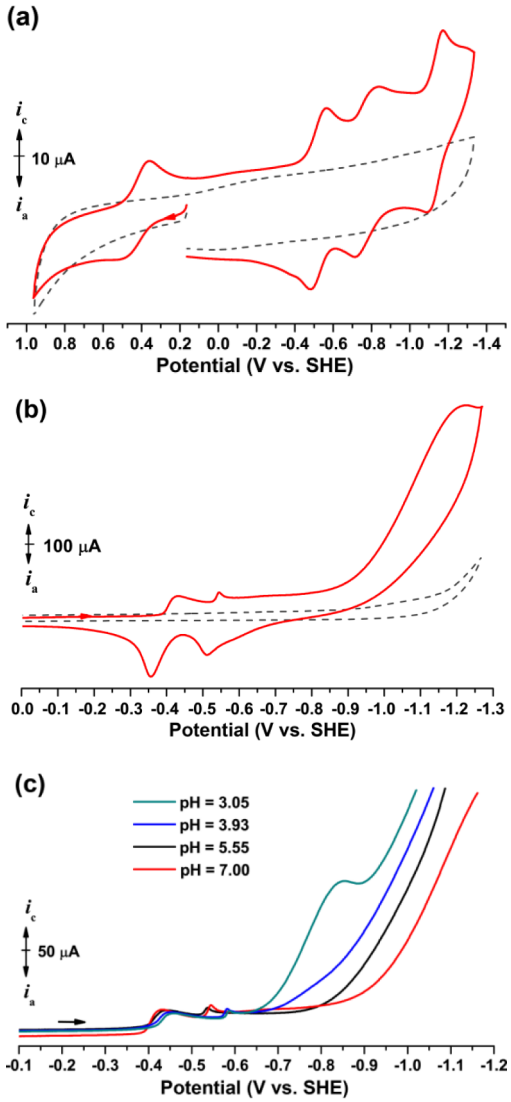

Figure 2. CVs in the presence (1 mM, red line) and absence (dashed line) of **6** at a scan rate of 100 mV/s: (a) DMF solution containing 0.1 M (n-Bu_4N)PF_6; (b) pH 7 phosphate buffer (0.1 M); and (c) cathodic scan of **6** (1 mM) in 0.1 M phosphate solution at various pH values.

with the square root of the scan rate and also with the concentration of **6** (Figure S11), indicating a diffusion-controlled process. It appears that the cobalt complex redissolves in water after it is oxidized to the [Co(ppq)-aqua]$^{2+}$ state.

The catalytic current illustrated in Figure 2b is considerably greater than the stoichiometric redox reactions described above. The onset of this catalytic current is clearly influenced by the solution pH (Figure 2c). For example, for a 200 μA catalytic current the applied potential declines linearly with increasing pH (Figure S12), evidencing the involvement of a proton in the initial stage of electrochemical catalysis. Meanwhile, there is an obvious potential gap between the onset of the catalytic current and the [Co(ppq)-aqua]$^{+}$/[Co(ppq)-aqua]^{0} redox event. From these observations we propose that reduction of [Co(ppq)-aqua]^{0} is a proton-coupled redox process, and the resulting cobalt hydride species leads to hydrogen generation. In fact, the current peak for [Co(ppq)-aqua]^{0} reduction can be distinguished from the catalytic current in the voltammogram at pH = 3.05 (Figure 2c). Under neutral conditions, the redox and catalytic currents fully overlap with each other. At pH 7.0, an onset overpotential (difference between applied and thermodynamic potentials) of 487 mV was estimated for catalytic proton reduction by **6**.

Encouraged by evidence that **6** can be a molecular electrocatalyst driving proton reduction in water, we looked at the utility of **6** in visible light-driven H_2 generation. $[Ru(bpy)_3]Cl_2$ was employed as a photosensitizer and ascorbic acid (AA) as a sacrificial electron donor in aqueous solution with **6** as the PRC. Previous studies have shown that similar three component systems demonstrate quenching of photo-excited $[Ru(bpy)_3]^{2+}$ by ascorbic acid, followed by reduction of the PRC by the generated $[Ru(bpy)_3]^{+}$ (Scheme 3).[14]

Scheme 3

$$[Ru(bpy)_3]^{2+} \xrightarrow{h\upsilon} [Ru(bpy)_3]^{2+*}$$

$$[Ru(bpy)_3]^{2+*} + AA \longrightarrow [Ru(bpy)_3]^{+} + AA^{+}$$

$$[Ru(bpy)_3]^{+} + H_2O \xrightarrow{PRC} 0.5\ H_2 + OH^{-} + [Ru(bpy)_3]^{2+}$$

In a typical experiment, a 33 mL round-bottomed flask was charged with 10 mL of aqueous ascorbic acid (0.3 mM, adjusted to pH = 4 with NaOH), $[Ru(bpy)_3]Cl_2$ (0.4 mM), complex **6**, and a stirring bar. The solution was degassed by bubbling Ar for 20 min, and then the flask was sealed with a septum cap. The absence of oxygen in the flask was verified by GC prior to light irradiation. The flask was placed in a water jacketed beaker controlled to 20 °C. The system was irradiated by a 18 module blue LED light strip (λ_{max} = 469 nm) wrapped around the beaker and connected to a 12 V power supply. The headspace gas was analyzed by GC every 30 min to determine the amount of generated hydrogen. Each experiment was repeated at least 3 times, and the average values as well as the associated uncertainties were calculated. The produced hydrogen vs time profiles at catalyst **6** concentrations ranging from 1 to 5 μM are displayed in Figure 3a. A plot of the initial rate of hydrogen generation vs catalyst concentration indicates the reaction is pseudo-first order in catalyst, and the observed rate constant is 586 h^{-1} (Figure 3b). This observed rate constant represents the turnover frequency (TOF) at catalyst concentrations below 5 μM. It is noteworthy that a much smaller TOF of 172 h^{-1} was observed when 20 μM catalyst was used, although more hydrogen was generated. The turnover number after 3 h blue light irradiation of a system containing 3 μM of **6** was determined to be 333. If **6** is replaced by $CoCl_2$-$6H_2O$, no H_2 evolution was observed upon irradiation, even at a relatively high concentration (20 μM) of the salt. This control experiment rules out any contribution of the simple cobalt cation to light-driven H_2 evolution.

In this study we have introduced a new polypyridine ligand capable of coordinating Co(II) in an approximate square planar environment. The resulting complex is soluble in water at pH = 7 and shows good stability even at lower pH. The complex is well-behaved electrochemically and shows a catalytic current for proton reduction at an onset potential of −0.73 V at pH = 3.93. Hydrogen production appears to involve a proton-coupled electron-transfer event. In the presence of a photosensitizer and a sacrificial electron donor (ascorbic acid), the same PRC evolves hydrogen when exposed to blue light. Future studies

dx.doi.org/10.1021/ja501257d | J. Am. Chem. Soc. 2014, 136, 4881−4884

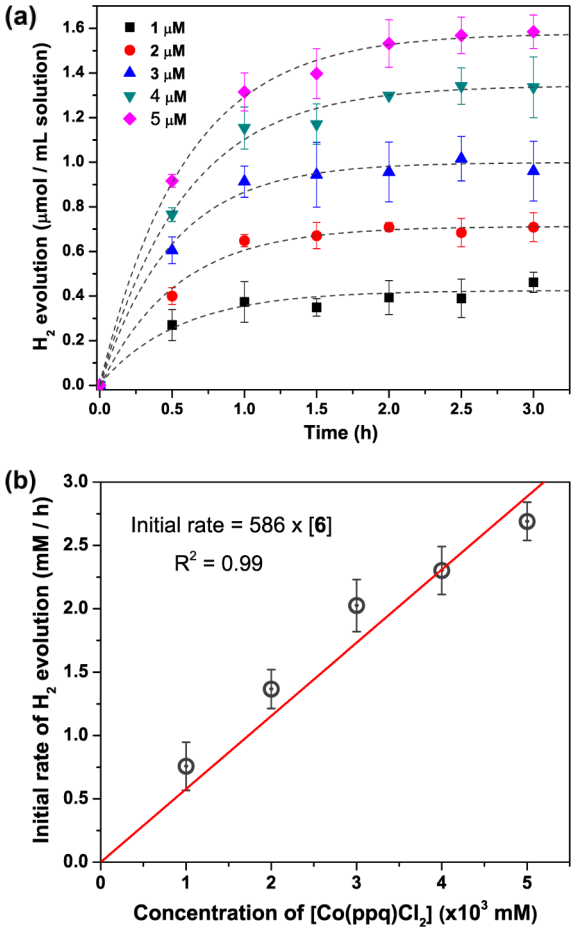

Figure 3. (a) Kinetic plots of light-driven H_2 evolution with [**6**] = 1 μM (■), 2 μM (●), 3 μM (▲), 4 μM (▼), 5 μM (◆) in a 0.3 M ascorbic acid solution (pH = 4) containing 0.4 mM $[Ru(bpy)_3]Cl_2$; the amounts of generated H_2 were given as an average of three independent measurements. (b) Initial rate of H_2 evolution (time = 0 h) versus [**6**].

will center on the mechanistic features of this and other closely related water reduction systems and also attempt to incorporate these systems into a dyad assembly containing both the PRC and the photosensitizer.

■ ASSOCIATED CONTENT

Ⓢ Supporting Information

X-ray crystallographic data for complex **6** in CIF format. Synthetic details, ^{1}H NMR, UV-vis, and electrochemical data. This material is available free of charge via the Internet at http://pubs.acs.org.

■ AUTHOR INFORMATION

Corresponding Author

thummel@uh.edu

Notes

The authors declare no competing financial interest.

■ ACKNOWLEDGMENTS

We thank the Division of Chemical Sciences, Geosciences, and Biosciences, Office of Basic Energy Sciences of the U.S. Department of Energy (grant DE-FG02-07ER15888) and the Robert A. Welch Foundation (grant E-621) for financial support of this work. We also thank Dr. Kristin Kirchbaum for assistance with the X-ray determination.

■ REFERENCES

(1) Eisenberg, R. *Science* **2009**, *324*, 44.
(2) Reece, S. Y.; Hamel, J. a; Sung, K.; Jarvi, T. D.; Esswein, A. J.; Pijpers, J. J. H.; Nocera, D. G. *Science* **2011**, *334*, 645.
(3) Barber, J. *Chem. Soc. Rev.* **2009**, *38*, 185.
(4) Artero, V.; Chavarot-Kerlidou, M.; Fontecave, M. *Angew. Chem., Int. Ed. Engl.* **2011**, *50*, 7238.
(5) Eckenhoff, W. T.; Eisenberg, R. *Dalton Trans.* **2012**, *41*, 13004.
(6) Chao, T.-H.; Espenson, J. H. *J. Am. Chem. Soc.* **1978**, *100*, 129.
(7) Fisher, B. J.; Eisenberg, R. *J. Am. Chem. Soc.* **1980**, *102*, 7361.
(8) Baffert, C.; Artero, V.; Fontecave, M. *Inorg. Chem.* **2007**, *46*, 1817.
(9) Jacques, P.-A.; Artero, V.; Pécaut, J.; Fontecave, M. *Proc. Natl. Acad. Sci. U.S.A.* **2009**, *106*, 20627.
(10) Stubbert, B. D.; Peters, J. C.; Gray, H. B. *J. Am. Chem. Soc.* **2011**, *133*, 18070.
(11) Hu, X.; Brunschwig, B. S.; Peters, J. C. *J. Am. Chem. Soc.* **2007**, *129*, 8988.
(12) McCrory, C. C. L.; Uyeda, C.; Peters, J. C. *J. Am. Chem. Soc.* **2012**, *134*, 3164.
(13) Artero, V.; Fontecave, M. *Coord. Chem. Rev.* **2005**, *249*, 1518.
(14) Creutz, C.; Sutin, N. *Coord. Chem. Rev.* **1985**, *64*, 321.
(15) Kellett, R. M.; Spiro, T. G. *Inorg. Chem.* **1985**, *24*, 2373.
(16) Sun, Y.; Bigi, J. P.; Piro, N. a; Tang, M. L.; Long, J. R.; Chang, C. J. *J. Am. Chem. Soc.* **2011**, *133*, 9212.
(17) Thoi, V. S.; Sun, Y.; Long, J. R.; Chang, C. J. *Chem. Soc. Rev.* **2012**, *41*, 8231.
(18) Singh, W. M.; Baine, T.; Kudo, S.; Tian, S.; Ma, X. A. N.; Zhou, H.; DeYonker, N. J.; Pham, T. C.; Bollinger, J. C.; Baker, D. L.; Yan, B.; Webster, C. E.; Zhao, X. *Angew. Chem., Int. Ed. Engl.* **2012**, *51*, 5941.
(19) Leung, C.-F.; Ng, S.-M.; Ko, C.-C.; Man, W.-L.; Wu, J.; Chen, L.; Lau, T.-C. *Energy Environ. Sci.* **2012**, *5*, 7903.
(20) Nippe, M.; Khnayzer, R. S.; Panetier, J. a.; Zee, D. Z.; Olaiya, B. S.; Head-Gordon, M.; Chang, C. J.; Castellano, F. N.; Long, J. R. *Chem. Sci.* **2013**, *4*, 3934.
(21) Chirik, P. J. *Inorg. Chem.* **2011**, *50*, 9737.
(22) Luca, O. R.; Crabtree, R. H. *Chem. Soc. Rev.* **2013**, *42*, 1440.
(23) Kaveevivitchai, N.; Zong, R.; Tseng, H.-W.; Chitta, R.; Thummel, R. P. *Inorg. Chem.* **2012**, *51*, 2930.
(24) Kohler, L.; Kaveevivitchai, N.; Zong, R.; Thummel, R. P. *Inorg. Chem.* **2014**, *53*, 912.
(25) Kaveevivitchai, N.; Kohler, L.; Zong, R.; El Ojaimi, M.; Mehta, N.; Thummel, R. P. *Inorg. Chem.* **2013**, *52*, 10615.
(26) Kaveevivitchai, N.; Chitta, R.; Zong, R.; El Ojaimi, M.; Thummel, R. P. *J. Am. Chem. Soc.* **2012**, *134*, 10721.
(27) Tseng, H.-W.; Zong, R.; Muckerman, J. T.; Thummel, R. *Inorg. Chem.* **2008**, *47*, 11763.
(28) Zong, R.; Thummel, R. P. *J. Am. Chem. Soc.* **2005**, *127*, 12802.
(29) Zhang, G.; Zong, R.; Tseng, H.-W.; Thummel, R. P. *Inorg. Chem.* **2008**, *47*, 990.
(30) Diedrich, C. L.; Haase, D.; Christophers, J. *Synthesis* **2008**, *14*, 2199.
(31) Morosin, B. J. *Chem. Phys.* **1966**, *44*, 252.
(32) Pagola, S.; Trowell, K. T.; Havas, K. C.; Reed, Z. D.; Chan, D. G.; Van Dongen, M. J.; DeFotis, G. C. *Inorg. Chem.* **2013**, *52*, 13341.